Advanced Materials Research Vol. 831 (2014) pp 321-325
© (2014) Trans Tech Publications, Switzerland
doi:10.4028/www.scientific.net/AMR.831.321

Costa, C.M.L., Zornberg, J.G., and Costa, Y.D.J. (2014). "Failure of Geotextile-Reinforced Walls in Centrifuge Model Tests," Advanced Materials Research, Advances in Civil Engineering and Building Materials III, Vol. 831, January, pp. 321-325.

Failure of Geotextile-Reinforced Walls in Centrifuge Model Tests

Costa, C. M. L[1, a], Zornberg, J. G.[2,b] and Costa, Y. D. J.[1, c]

[1]Federal University of Rio Grande do Norte, Lagoa Nova, Civil Engineering Department, 59015000, Natal, RN, Brazil

[2]University of Texas-Austin, Civil Engineering Department-GEO, 301 E. Dean Keeton, 78712-0280, Austin, TX, USA

[a] carina@ct.ufrn.br, [b] zornberg@mail.utexas.edu, [c] ydjcosta@ct.ufrn.br

Keywords: Geosynthetics, Geotextiles, GRS wall, Retaining Wall.

Abstract. This paper presents the results of centrifuge tests performed to investigate the behavior of geotextile-reinforced soil walls beyond stress conditions. The models were built using nonwoven fabrics as reinforcement layers and dry sand as backfill. Digital image analysis techniques were used to determine the displacement of sand markers placed along the reinforcements. The models were loaded until failure by increasing centrifugal acceleration, and the movements of the sand markers were used to determine the strain distributions along the reinforcement layers. The results revealed that stresses redistribute among reinforcement layers as models approach failure. Current design methods for GRS walls were found to be conservative when applied to predict the behavior of the reduced-scale models.

Introduction

Geosynthetic-reinforced soil (GRS) walls have been used successfully in Geotechnical Engineering in the past few years as a result of their technical and economical advantages. However many uncertainties remain regarding the behavior of this type of retaining wall structure. Conventional GRS wall design methods, for instance, include the assumption that the maximum force among all the reinforcement layers is located at the toe of the wall. This is due to the horizontal stress distribution assumed in conventional retaining wall structures, that is, growing linearly with depth. This distribution, however, is not always observed in GRS walls. Restrictions caused by the foundation of the wall as well as friction between the backfill soil and the wall face may cause different distributions.

Specifically with respect to centrifuge tests, few studies report reinforcement force distribution with wall depth. For illustration purposes, based on a literature review conducted by [1] that included 13 studies on centrifuge tests of reinforced soil structures, only the research carried out by [2] included measurements of force distribution in the reinforcement.

Although there are several instrumented geosynthetic wall case histories showing load distribution in reinforcement as a function of wall height, the monitored structures were under working stress conditions. There is practically no mention of reinforcement load distribution in the literature for centrifuge models of GRS walls beyond stress condition.

Accordingly, this paper presents the results of centrifuge model tests that allowed for the observation of GRS walls deformation under failure conditions.

Description of the centrifuge models tests

The centrifuge tests were performed using a 15 g-ton geotechnical centrifuge at the University of Colorado at Boulder. The models were built using dry sand as backfill and interfacing fabrics as reinforcements. The sand is a uniformly graded sand, classified as SP according to the Unified System. The reinforcement material is a 100% polyester fabric with an unconfined ultimate tensile strength of 0.033 kN/m [3].

A box with inside dimensions of 419 mm x 203 mm in plan, and 300 mm in height was used to house the models. A transparent Plexiglas was used as one of the side walls of the box to enable in-flight visualization of the models during testing.

Figure 1 shows the basic geometry of the models. The facing was extensible (i.e. wrapped-around reinforcements). The sand was pluviated though air to give a relative density of 70%. All models were built using reinforcements with 203 mm in length. The layer designation adopted herein is also showed in Fig. 1. Layer 1 corresponds to the bottom layer, whereas layer 12 indicates the top reinforcement layer.

The instrumentation of the models included one linear variable displacement transformer (LVDT) used to observe vertical settlement at the top of the model (Fig. 1). Black colored sand markers were placed along the Plexiglas wall at each reinforcement layer. The movement of the markers was monitored using a digital image acquisition system, which allowed for the determination of the strain distributions along the reinforcement layers. Further details of the model tests can be found in [4].

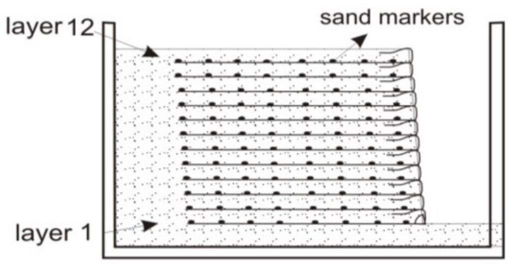

Fig 1. Layout of the models.

The models were loaded until failure increasing the centrifugal acceleration. The results of three identical centrifuge tests are presented in this paper.The first model is designated herein as models F1. The two additional tests (models F2 and F3) were conducted to evaluate the repeatability of the test results.

Procedure to Obtain Reinforcement Strain Distribution

The images collected from the acquisition system were analyzed using the same procedure described by [5]. For each reinforcement layer, the marker closest to the face was considered the reference point for determination of relative distances between markers. The displacement distribution data was fitted to the same sigmoid curve used by [6]. Eq. (1) shows the sigmoid function used to fit the displacements.

$$d = \frac{1}{a + b \cdot e^{-cx}} \tag{1}$$

Where d is the marker displacement at a given image, x is the distance between the marker and the corresponding reference marker, “e” is the natural logarithm base, and a, b, and c are parameters defined by fitting the displacement data to the sigmoid curve using least squares techniques.

The geotextile strain distribution was then calculated as the derivative of the displacement distribution function. Further details on this procedure can be found in [4, 5].

Centrifuge test results

G-level at failure (N_f) for models F1, F2 and F3 was 20, 19 and 21g, respectively. Figure 2 presents the strain distribution for model F3, layer 10. The *locus* of maximum strain (peak strain) for each reinforcement layer for a centrifugal acceleration equal to 95%N_f (point A, see Fig. 2) was used to locate the failure surface in the models. Figure 3 presents the location of failure surface for the models and demonstrates the good repeatability of the results

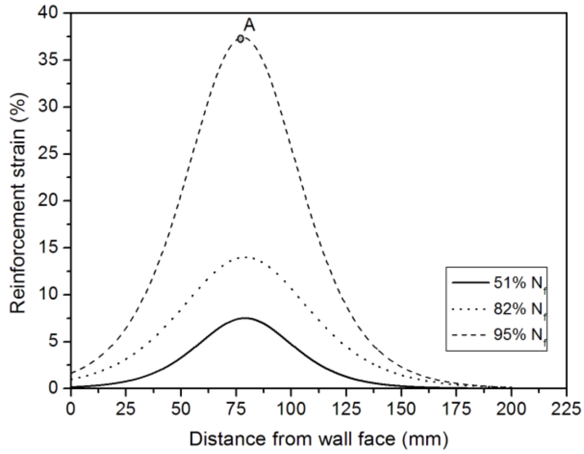

Fig. 2. Strain distribution for model F3, layer 10

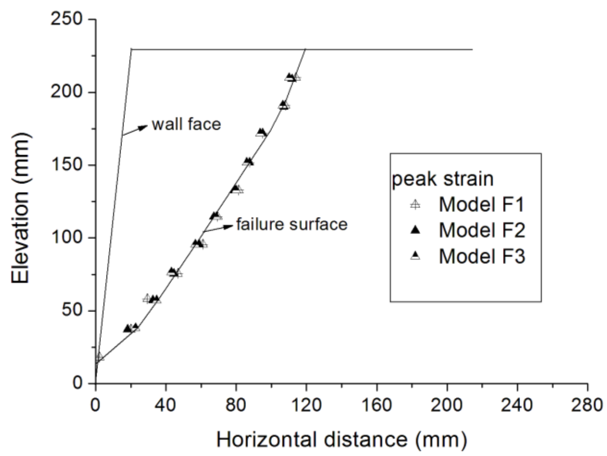

Fig. 3. Location of failure surface

Comparison between predicted and experimental results

The Tieback Wedge method was used to predict g-level at failure for GRS wall models. According to the method, the centrifuge acceleration at failure can be obtained as:

$$T_{max} = k_a \cdot N \cdot \gamma \cdot z \cdot S_v \tag{2}$$

Where Tmax is the maximum reinforcement tension for Layer 1 (unconfined geotextile tensile strength), Ka is the active lateral earth pressure coefficient, Ka= $\tan^2$ (45-ϕ/2), ϕ is the soil friction angle for plane strain conditions ($\phi = 42^0$), N is the scale factor (at failure conditions, N=Nf), γ is the dry unit weight of the soil (γ=16.08 kN/m^3), z is the depth below top of wall to reinforcement layer, and S_v is the vertical reinforcement spacing (S_v = 19.05 mm).

The g-level at failure for the models was about eight times higher than the value predicted using Eq. (2), this indicates that the Tieback Wedge method, currently adopted for GRS wall design was conservative.

The difference between predicted and experimental behavior of the tested models may have been caused by the increase in reinforcement tensile strength due to soil confinement and also by the stress redistribution between reinforcement layers.

The effect of confinement on tensile strength for the same geotextile used in this study was investigated by [1]. According to the author, the geotextile confined strength is about 3.7 times greater than the unconfined value. Incorporating the result obtained by [1] into the present study, the ratio between acceleration at failure (N_f) recorded for the models and the predicted acceleration (N_{fp}) based on Eq. (2) equals 2.

Another important aspect of the material used is that confined tensile strength of the geotextile seems to be the same, for different confining stress values in the models. This behavior was observed by other authors [1, 7].

Figure 4 illustrates the typical behavior obtained in the models for maximum strain (peak strain) for each reinforcement layer as a function of wall height. Reinforcement load could be obtained in Fig.3 using expression (3).

$$T=J\cdot\varepsilon \tag{3}$$

Where: T, J and ε, are the force, the secant stiffness and the reinforcement strain, respectively.

The confined stiffness value must be considered for the models, since literature findings, e.g. [8,9], show that reinforcement stiffness increases under soil confinement.

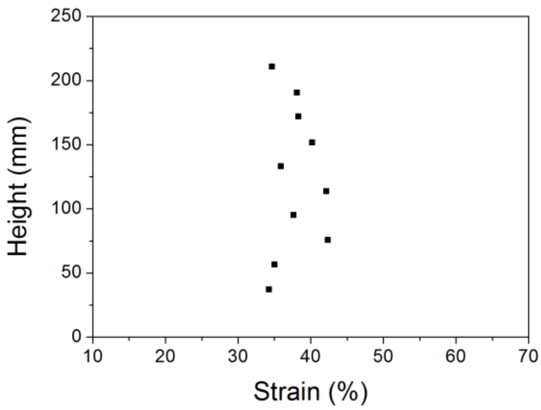

Fig. 4. Distribution of reinforcement peak strain with height for model F3

Based on Figure 4, it can be assumed that the maximum reinforcement force is constant with depth if reinforcement stiffness under confinement conditions is not significantly changed as vertical confining stress varies in the models. This hypothesis is consistent, since results described in the literature [e.g. 10] show that the most significant variation in stiffness with vertical confining stress applied to nonwoven geotextiles occurs for values of reinforcement strain less than 2%. Thus, the variation in stiffness with confining stress should be negligible for the models, since reinforcement strains are much greater ($\varepsilon>10\%$, see Fig. 4).

Studies performed by [1, 7] for the geotextile used in this study also indicate that the confined tensile strength of the geotextile did not vary significantly with the vertical stress variation in the models. Thus, confined stiffness likely has the same behavior.

Based on the results of the tensile tests conducted to the geotextile used in this study, the variation of peak strain with depth for N=95% N_f (Fig. 4) cause a negligible difference in reinforcement load. Thus, force distribution could also be assumed constant with wall depth for N=95% N_f. This behavior suggests that for failure conditions there is stress redistribution among reinforcement layers and the maximum reinforcement load is the same for each layer.

Conclusions

The use of traditional design methods for GRS walls for predicting g-level at failure of the models showed significantly lower values than that of the experimental results. The effect of confinement on the tensile strength of reinforcement should have contributed for this discrepancy. The peak reinforcement strain distribution with wall height, as models approach failure, suggest load redistribution between reinforcement layers. This redistribution tends to increase the discrepancy between predicted and experimental results.

Acknowledgments

The authors are grateful to the Brazilian Research Agency CAPES for the support provided to this research.

References

[1] Arriaga, F., 2003. Response of geosynthetic-reinforced structures under working stress and failure conditions, Ph.D. Thesis, University of Colorado at Boulder, Boulder, Colorado, USA, 205p.

[2] Jaber, M. B., 1989. Behavior of reinforced soil walls in centrifuge model tests. Berkeley, Ph.D. Thesis, University of California, Berkeley, 239p.

[3] ASTM D4595, Standard test method for tensile properties of geotextiles by the wide-width strip method, American Society for Testing and Materials,West Conshohocken, Pennsylvania, USA.

[4] Costa, C. M. L., 2004. Time-dependent deformations in geotextile reinforced soil walls, Ph.D. Thesis, School of Engineering at Sao Carlos, University of Sao Paulo, Sao Carlos, Sao Paulo, Brazil, 330p. (in Portuguese).

[5] Zornberg, J. G. and Arriaga, F., 2003, Strain Distribution within Geosynthetic-Reinforced Slopes. Journal of Geotechnical and Geoenvironmental Engineering, v. 129, n.1, 32-45.

[6] Zornberg, J. G., 1994, Performance of geotextile-reinforced soil structures. Ph.D. Thesis, University of California, Berkeley, California, USA.

[7] Zornberg, J. G., Sitar, N., and Mitchell, J. K., 1998, Performance of geosynthetic reinforced slopes at failure. Journal of Geotechnical and Geoenvironmental Engineering, v. 124, n. 8, 670-683.

[8] Wilson-Fahmy, R. F., Koerner, R. M. and Fleck, J. A., 1993, Unconfined and confined wide width tension testing of geosynthetics. In: Cheng, S. J. C. Geosynthetics soil reinforcement testing procedures. Philadelphia, p. 49-63.

[9] Ballegeer, J. P., Wu, J. T. H., 1993. Intrinsic confined and unconfined load-deformation properties of geotextiles. In: Cheng, S. J. C. Geosynthetics soil reinforcement testing procedures. Philadelphia. p. 16-31.

[10] Christopher, B. R., Holtz, R. D. and Bell, W. D., 1986, New tests for determining the in-soil stress-strain properties of geotextiles. Proceedings of the Third International Conference on Geotextiles, Vienna, Austria, 3, 683-688.